Formation of $(n\times1)$-O/Ag(110) overlayers and the role of step-edge atoms

W. W. Pai*
Department of Physics, University of Maryland, College Park, Maryland 20742

J. E. Reutt-Robey
Department of Chemistry, University of Maryland, College Park, Maryland 20742
(Received 18 December 1995)

Oxygen adsorption on Ag(110) was studied by ultrahigh vacuum scanning tunneling microscopy. Strong evidence that the $n\times1),n=7,\ldots,2$, oxygen overlayers adopt an ''added-row'' structure similar to the (2×1)-O/Cu(110) system is presented. Since the oxygen ''added row'' on Ag(110) is a -Ag-O-Ag- chainlike structure atop the original substrate, a source of the substrate atoms must exist. Steps, in principle, serve as an efficient source of these substrate atoms, provided that the detachment rates from the step edges are sufficiently large. The nominal detachment rate ($\sim$ 3 Ag atoms/s per step site) is sufficient to supply atoms to form the added-row structure when the oxygen partial pressure is low. For high oxygen pressures ($\sim P_{O_2}>10^{-5}$ mbar), the rate of dissociative oxygen chemisorption is competitive with the Ag supply rate from step detachments, and a second source of Ag atoms is provided by vacancy-island generation on the terraces. The microscopic structure of the oxygen overlayer of O/Ag(110) is quite similar to those of O/Cu(110) and O/Ni(110), but some differences in the formation kinetics are noted. [S0163-1829(96)06323-0]

I. INTRODUCTION

The mass transfer during complex surface processes such as film growth and chemical etching has long been a critical issue. Mass transport is not a phenomenon limited to those complicated situations, however. Recent studies have pointed out that the substrate atoms play an active and direct role in ''elementary'' surface processes such as chemisorption.[1] Rapidly developing microscopic techniques such as scanning tunneling microscopy (STM), atomic force microscopy, low-energy electron microscopy, and reflection electron microscopy allow us to study this fundamental issue.

Our specific goal is to establish the relationship between the change in surface morphology and the adlayer formation through the mass transport mechanisms. This study focuses on the O/Ag(110) system. As briefly reported elsewhere,[2] O adopts an added-row configuration in which extra Ag atoms are incorporated to form a chainlike -Ag-O-Ag- structure. The predominant source of Ag adatoms is the step edge. At O pressure below 10^{-5} mbar, the step edge is sufficient to supply Ag atoms for the formation of added rows. However, at O pressure above 10^{-5} mbar, another significant source, i.e., the vacancy-island formation, is found to supplement the Ag source from step edges, sustaining the overlayer formation process.

In this paper we report on a detailed examination of the added-row structure and stability. We show that the added-row structure is adopted for all $(n\times1)$-O phases, and that the manner in which the -Ag-O-Ag- rows terminate strongly affects the chain stability. The correspondence between the overlayer formation and the displacement of an isolated step is revisited, and the estimation of adatom density on the clean Ag(110) surface is confirmed. Finally, the step-edge supply under different oxygen dosing pressures is addressed in greater detail. In addition to the simple kinetic balance between the O adlayer formation rate and step-edge Ag supply rate, other complicating processes are discussed.

II. EXPERIMENT

Experiments are performed on a single-crystal silver surface with a macroscopic surface orientation within 0.1° of the (110) plane. All sample cleaning and STM experiments are performed in an ultrahigh vacuum apparatus that has been described previously.[3,4] After a lengthy initial sample cleaning,[3] the following treatment proved effective. The sample was first oxidized at 675 K ($P_{O_2}\sim5\times10^{-7}$ mbar), flashed to 800 K for 60 s, and then cooled to room temperature at a rate of 4 K/min. This procedure produced a large surface region (>5 mm across) with steps routinely separated by terraces of 1000 Å width. Tunneling conditions typically involved a sample bias from -1.0 to -2.5 V and a tunneling current 1.0–3.0 nA. Thermal drift was minimized (~0.5 Å/min) after a 20-h cooldown period. Mechanically cut Pt-Rh(30%) alloy tips were used. Occasional field emission on the tip helps to improve the tunneling condition. The sample is dosed with oxygen by backfilling the chamber through a Varian leak valve. Images presented in this paper were postprocessed with background subtraction and/or contrast adjustment.

III. RESULTS AND ANALYSIS

A. O/Ag(110) overlayers

1. Microscopic structure: Added rows

As found in previous studies, oxygen atoms arrange into long chains along [001] on this surface. A series of $(n\times1)$ ordered oxygen overlayers appears with increasing oxygen coverage, where $n=7,6,\ldots,2$.[5] The chain structure is indicative of a highly anisotropic interaction, e.g., strong at-

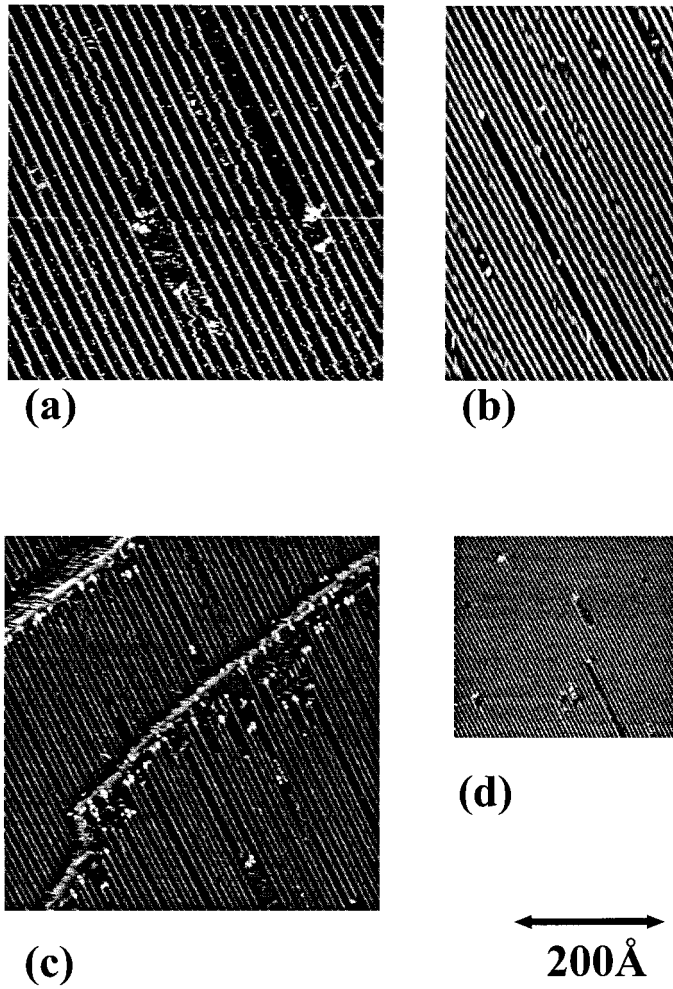

FIG. 1. O/Ag(110) overlayers of different nominal chain densities. (a) (7×1)-O structure, $\theta\sim1/7$. (b) (4×1)-O, $\theta\sim1/4$. (c) Mixture of (3×1)-O and (4×1)-O. (d) (2×1)-O. All four images are shown with the same scale for direct comparison.

tractive interactions along [001] and repulsive interactions along $[1\bar{1}0]$. The spatial distribution of the oxygen chains spans the surface and does not show preference to form at near-step regions. The oxygen overlayer often displays variations in the oxygen chain densities.[6] Figure 1 shows the oxygen overlayers at different oxygen densities. An area covered by mixed (3×1) and (4×1) oxygen chain densities is shown in Fig. 1(c).

To probe the microscopic structure of these rows, we first show these ''oxygen'' rows actually consist of both oxygen and silver atoms. The identification of the registries of the O and Ag atoms is possible with atomically resolved STM image as shown in Fig. 2(a). In this image, atoms are atomically resolved along the oxygen chains and the substrate silver rows are also resolved across the corrugated [001] direction. The bias-independent positions of the bright spots along the chains sit above the $[1\bar{1}0]$ substrate rows. These bright spots are assigned to O atoms, rather than Ag atoms, because the Ag atoms should seek the fourfold fcc sites rather than the short twofold bridge sites. However, earlier surface extended x-ray absorption fine-structure spectroscopy and inelastic He scattering experiments[7–10] place the O atoms in the long twofold bridge sites of Ag atoms along [001]. To reconcile this local geometry (O atoms in long twofold bridge) with our STM image (O atoms above close-packed rows), extra Ag atoms are needed to occupy fcc sites between the O atoms and the surface plane. This chainlike structure, dubbed an ''added row,'' was first confirmed on O/Cu(110) (Ref. 11) and then reported for O/Ni(110).[12] A schematic drawing of both the top and side views of this ''added-row'' structure is given in Fig. 2(c).

Further evidence that the O/Ag(110) system adopts this added-row structure is provided by the retraction of isolated steps upon oxygen exposure. As shown in Fig. 3, exposure to 300 L ($1\text{L}=10^{-6}$ Torr s) of oxygen causes an isolated step (more than 3000 Å from its neighbors) to move by 200 Å and an (8×1)-O overlayer to form on the terraces. During this retraction the step is pinned by impurity atoms, introducing a curvature to the step edge. The manner in which the step wraps about the pinning site[3] confirms that the step is retracting and thus acting as a source of Ag atoms.

The local registry of the atoms in a single oxygen chain is independent of the density of the oxygen overlayer. The O atoms of a (7×1) phase, shown in Fig. 4, assume the same registry as those of a (2×1) phase, shown in Fig. 2(a). The O atoms were imaged with STM as protrusions with Pt-Rh(30%) tips, regardless of tunneling voltage. The positions of the bright dots (O atoms) remain the same even if the polarity of the tunneling voltages is switched between the consecutive scans. The corrugation of the O rows, however, is sensitive to the tip conditions and the tunneling parameters. The corrugation along the [001] oxygen row in Fig. 4,

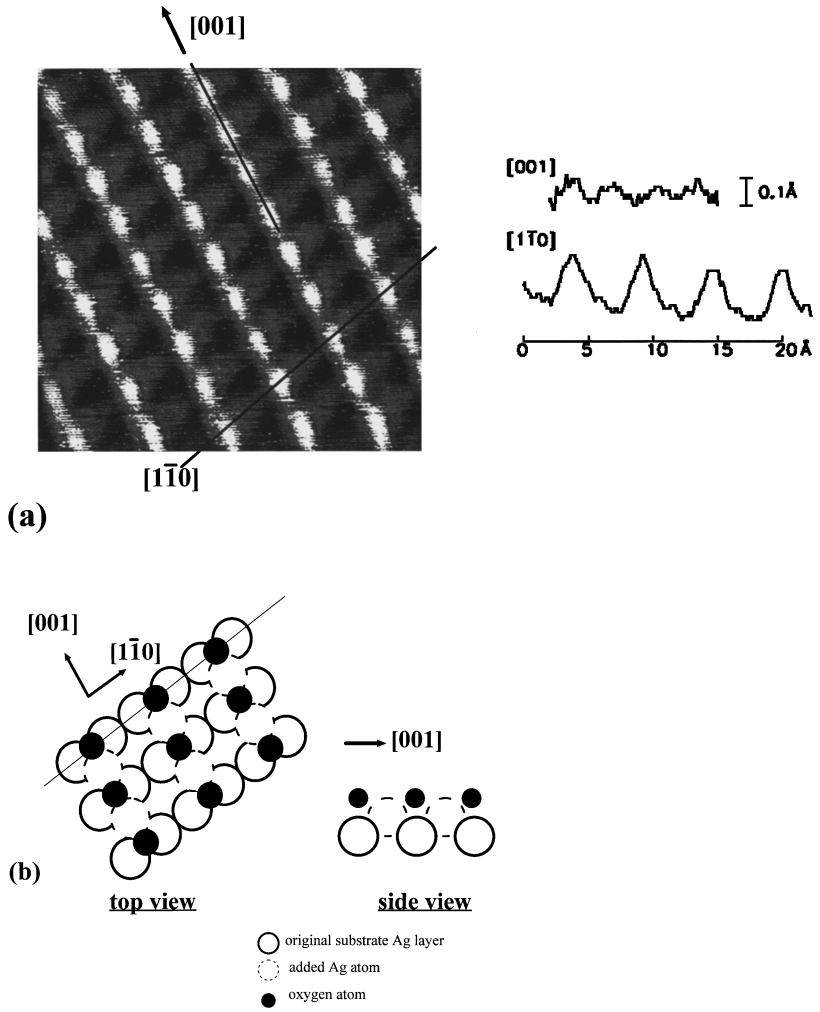

FIG. 2. (a) A 30 Å$\times$30 Å STM image of (2×1)-O/Ag(110) showing the ''added-row'' structure. Oxygen atoms are imaged as bright dots. The corrugation of the O overlayer along [001] and [1$\bar{1}$0] is also shown. Tunneling parameters are sample bias $V_t=-1.96$ V, tunneling current $I_t=2.16$ nA. (b) Schematic drawing of the ''added-row'' structure. Oxygen atoms (solid dark circles) incorporate the ''added'' Ag atoms (dashed circles) to form -Ag-O-Ag-chains. In the side view, O atoms are placed above the plane of added Ag atoms. The line is a guide to the eye for the bias-independent registry of Ag and O atoms.

taken with a bias voltage -0.46 V and a tunneling current 2.02 nA, is $\sim$0.2 Å . As shown in Fig. 2(a), however, a far smaller 0.08-Å corrugation is observed with tunneling parameters -1.96 V and 2.16 nA. Due to the sensitivity of the corrugation to the tunneling conditions, reliable information on the position of oxygen atoms above the surface plane cannot yet be drawn from the STM study. The data, nonetheless, place the O atoms above the top Ag plane. This result is consistent with a recent total-energy calculation based on an optimized added-row structure that shows the positions of O atoms are above the top Ag layer by as much as 0.59 Å for a (2×1) structure.[13,14]

2. Stability of the added rows: Chain fluctuations

The added rows fluctuate substantially at room temperature. These rows generally appear ''segmented'' in STM images [Fig. 5(a)]. This is attributed to the collective motion of the whole oxygen chain, rather than an actual ''breakup'' of the chain.[11] The ''frizzy'' appearance of the O chain is an effect of image acquisition caused by the near equivalence of the scanning time and the jumping time of the O chain. It has been suggested previously that the observed fluctuations of

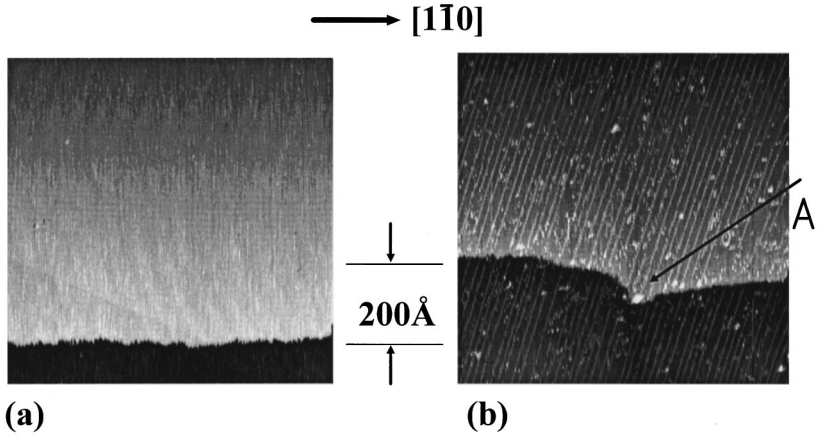

FIG. 3. 1000 Å$\times$1000 Å STM images showing the retraction of an isolated step: (a) The surface prior to oxygen exposure. (b) After $\sim$300-L O_2 exposure at a pressure of 10^{-7} mbar. The step on the clean surface retracts by $\sim$200 Å as an $\sim(8\times1)$-O overlayer forms. At point *A* the step is pinned by an impurity during retraction. The step bends towards the upper terrace, revealing evaporation of adatoms from the step edge. The nonorthogonality of the [1$\bar{1}$0] step and [001] oxygen chains is artificially caused by the coupling between *x* and *y* piezos of the STM.

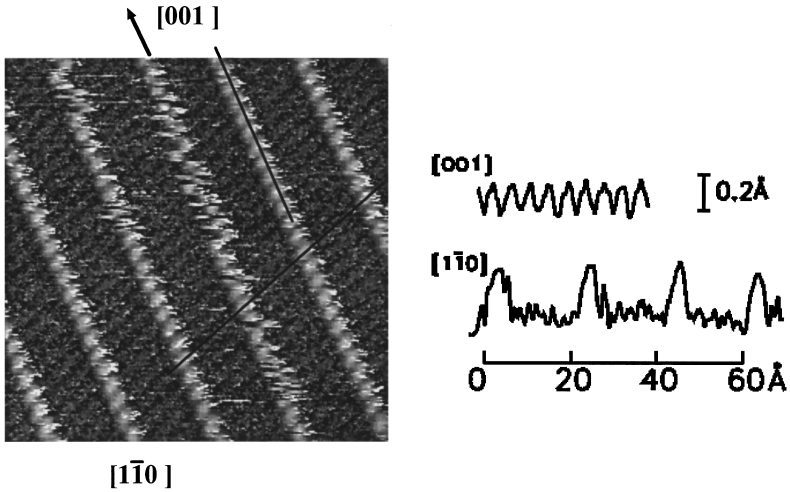

FIG. 4. A 100 Å×100 Å STM image of the (7×1)-O/Ag(110) phase showing the ''added-row'' structure. As shown in Fig. 2(a), O atoms are imaged as bright dots with a bias-independent registry. The corrugation of the O overlayer along [001] and [1$\bar{1}$0] are also shown. Tunneling parameters are sample bias $V_t = -0.46$ V, tunneling current $I_t = 2.02$ nA.

the O chains on Ag(110) are due to the existence of energy-degenerate sites.[6] While this effect may be important at higher chain densities, at low oxygen chain densities [$<(6\times1)$], a fluctuating O chain is not necessarily in an energy-degenerate site. Yet, the O chains appear quite mobile at these lower coverages. In general, we find that for the chain to gain stability (thus appear straight), the O chains must be ''pinned'' in some way. In Fig. 5(b), we show three chain-pinning mechanisms: (1) attaching the chain ends to impurities (shown in the two right circles), (2) attaching the chain ends to the lower side of the step (shown in the middle two circles), and (3) attaching to another chain across the step edge (shown in the very left circle).

B. The displacement of isolated steps and equilibrium Ag adatom concentration

Convincing confirmation of the added-row structure for O/Cu(110) and O/Ni(110) was provided by the step movements that accompanied oxygen exposure. Since the added rows require extra substrate atoms to form, the steps are expected to supply these atoms and retract during oxidation. Although the same argument applies to O/Ag(110), several factors may complicate the O/Ag(110) system. As we reported earlier,[4] the vicinal Ag(110) surfaces facet upon oxygen exposure. The step motion during faceting is rather complicated because large amounts of Ag atoms are transported across steps, with some steps advancing and others retracting during faceting. It is thus hard to single out the step motions caused by added-row formation. Since the typical size of a facet is several hundred angstroms, steps more widely separated than the facet size are needed to observe the step retractions induced by added-row formation alone.

We thus examine the displacement of an ''isolated'' step during oxygen exposure. An ''isolated'' step is defined rather arbitrarily as a step at least 3000 Å away from neighboring steps. The large terrace width is chosen to exclude the possibility that the neighboring steps are acting as atom ''sinks'' or ''sources'' otherwise. The step-step interactions and mass exchange between the isolated step and other steps (important for faceting) are thus negligibly small. We attribute the change of the position of this ''isolated'' step after oxidation exclusively to the added-row reconstruction. The step positions before and after oxygen exposure of one such ''isolated'' step are now compared. The preoxygen step position, shown in Fig. 3(a), retracts 200 Å after ~300-L oxygen exposure to a postoxygen position, as shown in Fig. 3(b). Meanwhile, an (8×1)-O overlayer is formed on the terraces. The *retraction* of this isolated step verifies that the step is an atom *source* and the oxygen overlayer structure incorporates extra Ag atoms. The immobile pinning site, also observed in Fig. 3(b), permits calibration of the thermal drift of the STM. The total thermal drift during the 50-min lapse between Figs. 3(a) and 3(b), 20 Å , is much smaller than the observed 200-Å step retraction.[15]

From these measurements of step retraction, one can estimate the equilibrium density of mobile silver atoms on the terrace of *clean* Ag(110). This is accomplished by comparing the distance a step retracts upon oxygen exposure to the coverage of the nascent oxygen overlayer. Since the stoichiometry of the added-row structure requires 1 Ag atom per O atom, any discrepancy between step-edge retraction and oxygen coverage must be accounted for by mobile Ag adatoms. In Fig. 3, the terrace width on either side of the step is 3000 Å. The 200-Å retraction of the step edge produces just enough silver atoms (0.07 ML) to support a (15×1) oxygen overlayer. A much higher density (8×1)-O structure with a 0.12-ML coverage is observed. Hence, the initial Ag adatom density is estimated to be 0.05 ML. Similarly, an isolated step spaced ~3800 Å away from the neighboring step retracted 310 Å after ~300-L O_2 exposure at 1×10^{-7} mbar. A (7×1)-O structure on the terraces was formed (see Fig. 6). Using the same arguments, an equilibrium Ag concentration of 0.06 ML on clean Ag(110) at room temperature is found. Finally, measurement of the step displacement of a (7×1)-O/Ag phase with ~1000-Å-wide terraces gives an adatom density of ca. 0.065 ML. Thus, three independent measurements yield Ag adatom concentrations of 0.058 ±0.008 ML.

The estimate of Ag density, evaluated by dividing the amount of step retraction to the width of the adjacent terrace, is valid in the simplest case that Ag adatoms completely go to the lower (or upper) terrace. What if the Ag adatoms detaching from steps can go in both step-up and step-down directions? We can generalize this estimate of the adatom density to these more complicated situations by making the assumption that the number of Ag atoms supplied onto a

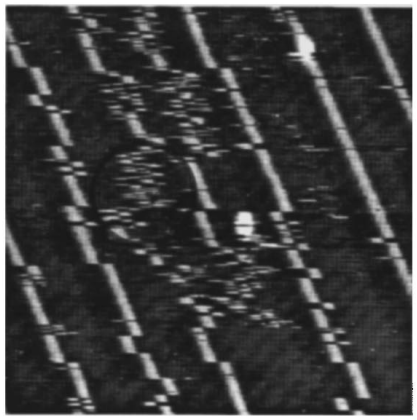

(a)

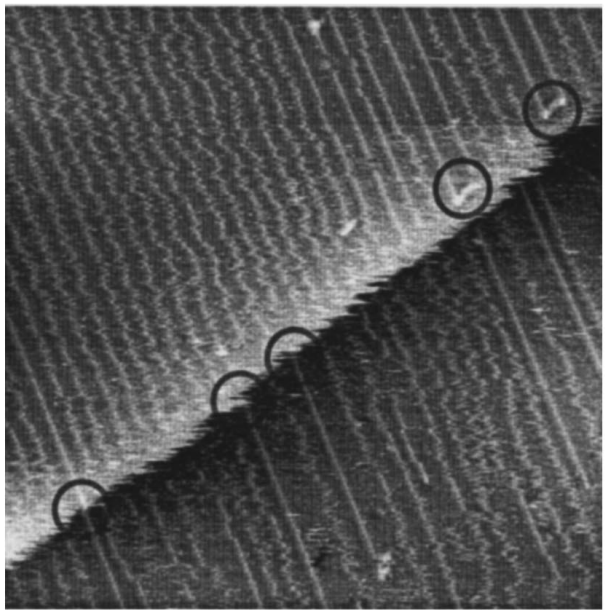

(b)

FIG. 5. (a) The collective motion of added rows causes the chains to appear ''segmented'' in this 100 Å$\times$100 Å STM image. Substantial fluctuations of the chains are observed. The chain is capable of jumping between neighboring sites on the time scale (500 ms) for a single scan line, as indicated in the gray circle. (b) The mobility of O chains can be reduced by three mechanisms: (1) attaching the chain ends to impurities (shown in the two right circles), (2) attaching the chain ends to the lower side of the step (shown in the middle two circles), and (3) attaching to another O chain across the step edge (shown in the very left circle). Image size 500 Å$\times$500 Å .

terrace is proportional to its terrace width. This assumption is valid if the following two conditions are met. First, the mass transport must allow fast distribution of Ag adatoms on terraces. Our measurements of oxygen-induced faceting[4] and step fluctuations[16] clearly show that transport across terraces is not diffusion limited. Secondly, the Ag adatoms detached from steps must be largely confined to adjacent terraces. This assumption—that Ag adatoms do not jump over neighboring steps—is reasonable because the activation energy for hopping across the step edge is expected to be larger than that for terrace diffusion.[17] Furthermore, given the low oxygen pressures ($<10^{-7}$ mbar) used in these experiments, the system remains in quasiequilibrium. The Ag adatom density and the chemical potential on different terraces are thus expected to be equal, and the driving force for Ag atoms to jump across terraces should be very small.

Our method for evaluating Ag adatom densities is now summarized. As shown in Fig. 7, the steps on the clean surface, positioned at $l_0,l_1,l_2,\ldots,$ are displaced by $d_0,d_1,d_2,\ldots$ upon oxygen exposure. The Ag adatom densities released onto the adjacent terraces are $\rho_0,\rho_1,\rho_2,\ldots$. The Ag adatom densities ρ_n, along with the initial equilibrium concentration, support the formation of added-row structures. To be quantitative, we next assign the relative probability for a Ag adatom to detach from a step onto an upper and lower terrace as α and β, respectively. Assuming the amount of Ag atoms supplied onto a terrace is proportional to its width, the retraction distance d_1 of one isolated step consists of two contributions: adatoms going to the upper terrace, αl_1, and adatoms going to the lower terrace, βl_2, i.e.,

$$d_1=\alpha l_1+\beta l_2,\quad d_2=\alpha l_2+\beta l_3,\ldots,\quad d_n=\alpha l_n+\beta l_{n+1}. \tag{1}$$

The Ag concentration supplied by steps onto l_1 terraces is simply

$$\rho_1=\frac{\beta l_1+\alpha l_1}{l_1}=\alpha+\beta. \tag{2}$$

Experimentally, we chose an isolated step with *equal* initial terrace widths, making $l_1=l_2$. This reduces Eq. (1) to $d_1=\alpha l_1+\beta l_1=\alpha l_2+\beta l_2=(\alpha+\beta)l_1$ (or l_2), and the Ag density can indeed be evaluated by simply dividing d_1 by l_1 (or l_2). Finally, we note that the Ag *equilibrium* adatom density, as obtained by subtracting the Ag density ρ released by the steps from the Ag density in the nascent oxygen overlayer, is a lower bound, as residual Ag adatoms may yet remain on the $(n\times1)$-O-covered surface.

C. Oxygen overlayer formation kinetics

In the preceding paper, which analyzes the thermal step fluctuations,[16] we concluded that Ag atoms exchange between steps and terraces with a nominal exchange rate of 3 Ag atoms/s per step site. Thus, even at room temperature, the step edge acts as a source of mobile silver adatoms. The existence of these adatoms and their quick exchange with the step edge indicates the step edge might be able to maintain the *equilibrium* concentration of (presumably highly reactive[18]) adatoms on the terraces as the oxygen overlayer forms. Since the oxygen overlayer requires a source of Ag adatoms, the efficiency of steps as adatom sources profoundly influences the kinetics of oxygen overlayer formation, as discussed below.

1. Rate-limiting case: Oxygen-induced ''pit formation''

We have shown that a substantial Ag concentration ($\sim$0.05 ML) exists on the surface, and that this equilibrium

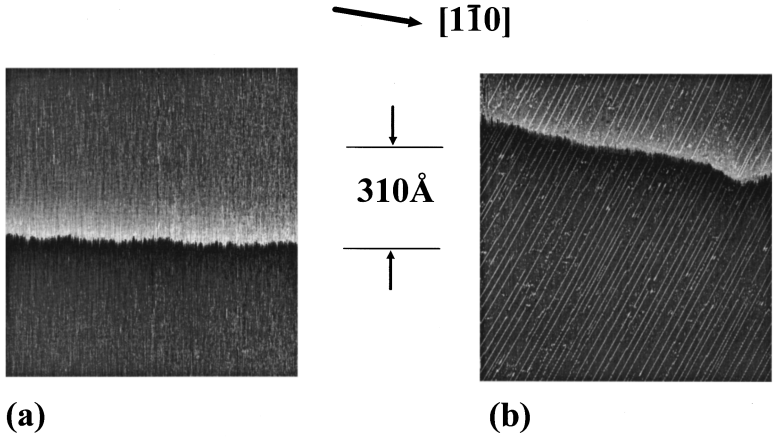

FIG. 6. 1000 Å×1000 Å STM images showing the retraction of an isolated step: (a) The surface prior to oxygen exposure. (b) After ~300-L O_2 exposure at $P_{O_2}\sim10^{-7}$ mbar. The step on the clean surface retracts by ~310 Å (between the *mean* step positions) as a ~(7×1)-O overlayer structure forms. The difference between the number of Ag atoms in the (7×1)-O phase and 310-Å retraction distance is accounted by the Ag equilibrium density of ~ 0.06 ML.

concentration can be maintained by the step-terrace exchange rate (ca. 3 atoms/s per step site). One might, therefore, imagine extrapolating to a sufficiently high oxygen dosing pressure, at which the Ag supply rate from the steps cannot keep up with the oxidation rate. In this case, either the oxidation process would gradually cease or a second supply channel of Ag atoms would be found. We now test the existence of this additional source of Ag atoms. By systematically increasing the oxygen dosing pressure, we challenge the ability of the steps to maintain the equilibrium concentration of Ag adatoms. Since the consumption of Ag adatoms will increase with oxygen pressure, at a sufficiently high pressure the adatom concentration will drop well below equilibrium. If the added-row reconstruction is to continue to form, another source of adatoms must be found.

Experiments with higher oxygen dosing pressures clearly reveal this secondary Ag adatom source. As shown in Fig. 8, at oxygen pressures above 10^{-5} mbar, pits start to form on the terraces. Large pits with diameters of several hundred Å are observed on large terraces after exposure of 300-L O_2 at $P_{O_2}=10^{-5}$ mbar. This remarkable morphological change indicates that adatoms are extracted from the substrate even at room temperature. Since the activation energy for substrate extraction does not depend upon oxygen pressure, we presume that substrate extraction occurs even at low oxygen pressures. Moreover, the formation of these large vacancy islands indicates that the upward detachment rate is appreciable, at least under these higher oxygen pressures. Since direct evidence for substrate extraction (i.e., the observation of pits) is not found at low oxygen pressures, such unstable pit structures must be filled by mobile Ag adatoms, apparently at a rate faster than the data acquisition rate of our STM. At higher oxygen pressures, however, when the density of mobile adatoms is depleted, terrace vacancies created by substrate extraction survive to nucleate the formation of large pits, providing a significant alternative source of Ag adatoms.

We can estimate the critical pressure P_c at which large pits should be expected to begin to form. We first assume that at P_c all Ag adatoms on terraces react with incoming O atoms to form Ag_2O nuclei before extra Ag atoms detach from the step edge. Equivalently, we assume that the density of O atoms adsorbed during the detachment time interval τ_a is comparable to half of the initial density, $n=0.05$ ML, of silver adatoms on the terrace:

$$\frac{n}{2}(\text{Langmuir})\approx 2P_cS_O\tau_a, \tag{3}$$

where $S_O=0.006$ (Refs. 5 and 19) is the initial sticking coefficient of O_2 (which is multiplied by a factor of two to account for the stoichiometric yield of O atoms), and $\tau_a=350$ ms, as reported above. Substituting these values into Eq. (3), we determine that the critical pressure is $\sim10^{-5}$ mbar, in good agreement with the observed critical pressure.

2. Non-rate-limiting case: Initial O overlayer formation below P_c

We interpret this pit formation as the result of the kinetic balance between two competing processes—the oxidation rate and the step-edge supply rate. Nice agreement is found for the value of the ''critical pressure.'' This further implies that the rate of oxygen overlayer formation will not be limited by the rate of Ag atom detachment from the step edge at typical dosing pressures ($<10^{-5}$ mbar). This can be tested

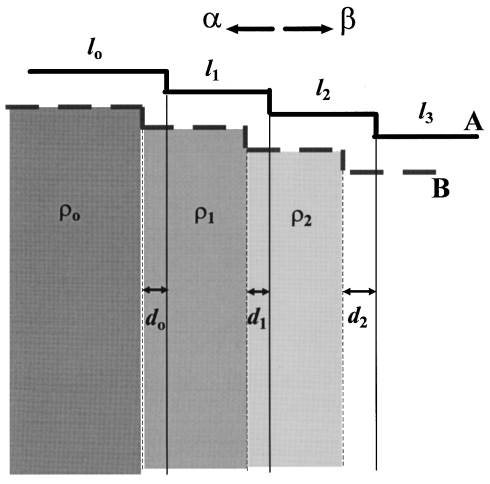

FIG. 7. Schematic illustration of step retraction. The initial surface (A) is an array of steps separated by terrace widths l_1,l_2,l_3. The surface after oxygen exposure (B) shows the steps retracted to new positions, with shifts of d_0,d_1,d_2. The Ag densities released by these step retractions onto terraces l_0,l_1,l_2, respectively, are designated ρ_0, ρ_1, and ρ_2. The relative probabilities for a Ag adatom to jump to upper and lower terraces are designated α and β, respectively.

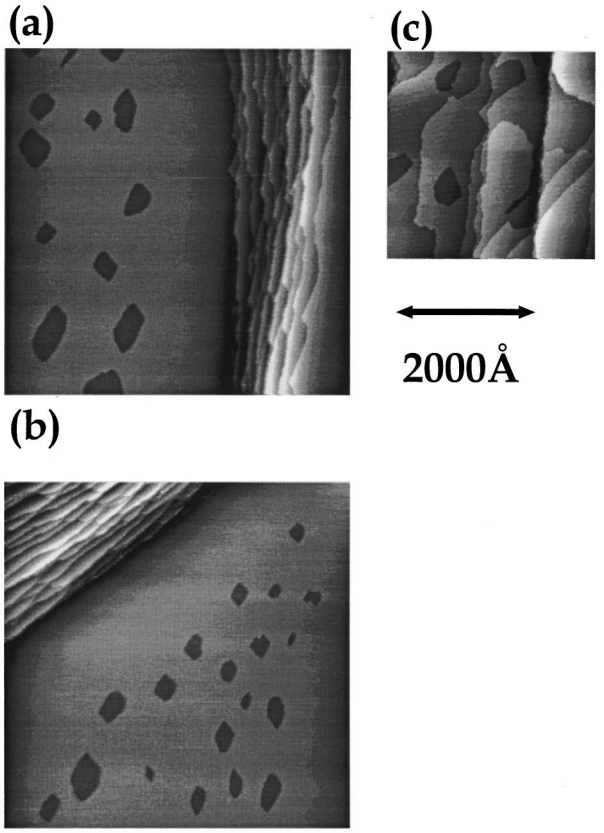

FIG. 8. Pit structures observed upon exposure to high O_2 pressures. (a),(b) Large area (5000 Å$\times$5000 Å) STM images upon exposure to $\sim$500 L O_2 at 10^{-5} mbar. Note the $\sim$1600-Å wide zone near step edges devoid of vacancy islands and the absence of pits in higher step density regions. (c) Pits are found occasionally on intermediate terraces ($\sim$1000 Å wide) as shown in this 3000 Å$\times$3000 Å STM image of an Ag(110) surface exposed to $\sim$300-L O_2 at 10^{-5} mbar. The large (400–700 Å diameter) pits formed under such high oxygen pressure exposure provide an additional Ag adatom source needed for the added-row reconstruction. Added rows decorate the pits.

by monitoring the speed with which the step retracts during oxygen adsorption. Using the time interval between successive detachments of $\tau_a=350$ ms, we can estimate the minimum time it should take for the step edge to retract by 200 Å and produce the overlayer structure of Fig. 3. From this maximum speed of $a_0/\tau_a\sim(4$ Å$)/(350$ ms) and assuming that all detaching atoms and preexisting mobile Ag adatoms react to form the oxygen overlayer, we determine that a step can retract 200 Å in as little as 18 s. This time is much shorter than the actual 50 min taken for the step-edge retraction and (8×1)-O overlayer formation. Indeed, in the first 18 s, the added rows were not yet formed and the step retraction speed was considerably less than the detachment rate a_0/τ_a. The detachment of Ag atoms from steps thus cannot be the rate-limiting step of added-row formation, at least at the *initial* stage when the oxygen density on the surface is rather low.[20] We believe the rate-limiting step involves the nucleation of oxygen chains of a certain minimum chain length.

IV. DISCUSSION

We have presented five main results: (1) $(n\times1)$-O/Ag(110) adopts an added-row structure. (2) A significant adatom density ($\geqslant0.05$ ML) exists on the surface. (3) Ag atoms are exchanging between steps and terraces with a rapid rate of $\sim$ 3 atoms/s per site. (4) A ''critical pressure'' is found, above which vacancy islands are generated. (5) Detachment from steps does not limit the rate of oxygen overlayer formation at low dosing pressures. We now further consider issues of equilibrium Ag adatom density and the mechanism for ''pit formation.'' A final perspective is provided by comparing this system to previously reported results for O/Cu(110) and O/Ni(110).

A. The equilibrium Ag adatom density

The equilibrium adatom density on terraces is determined by the free-energy difference between atoms on terrace sites and in the bulk. An adatom density $n\sim0.05$ ML, where $n=\exp(-\Delta G_f/kT)$, indicates the free-energy difference ΔG_f is only $\sim$0.07 eV.[21] This number is surprisingly small. Is this value plausible? From the embedded-atom method and equivalent crystal theory, it is found, incorrectly, that the Ag(110) surface will reconstruct.[22,23] Nevertheless, this is a good indication that the step creation energy, as well as the free-energy difference between atoms at terrace sites and in the bulk, should be rather small. Clean unreconstructed Ag(110) is also known to undergo a missing-row reconstruction under minor perturbation,[24,25] indicating an extrinsically metastable surface.

We emphasize that the equilibrium adatom concentration and the mass transport at step edges need not be directly correlated. Since the adatom density on terraces is an equilibrium property, it might not be maintained if the detachment from steps is kinetically limited. Conversely, a large mass flux between steps and terraces does not necessarily imply a high density of adatoms because of fast diffusion and efficient reattachments. We thus caution that the equilibrium density and mass transport mechanisms at steps require independent evaluation. In the present case, the efficient step-terrace exchange rate supports at high equilibrium concentration.

B. Pit formation mechanisms

Pit formation is observed only if the pressure is above a ''critical'' pressure $P_c\sim10^{-5}$ mbar. With the same oxygen net exposure, but delivered at lower oxygen pressures, the vacancy islands are not found on the surface. Moreover, the pits are not observed with a dosing pressure greater than P_c if the surface is previously covered with a dilute oxygen overlayer. The steps appear ''roughened'' instead (Fig. 9). The formation of a pit is apparently inhibited by an existing oxygen overlayer.

Experimentally, the majority of pits are observed on large terraces with terrace widths $\geqslant$2000 Å. The tendency to form pits on large terraces is attributed to two factors. First, Ag atoms detaching from steps will take longer to diffuse across larger terraces, as evidenced by the observed $\sim$1600-Å-wide ''depletion zone'' near step edges [see Figs. 8(a) and 8(b)]. Second, from Eq. (3), it follows that the detachment

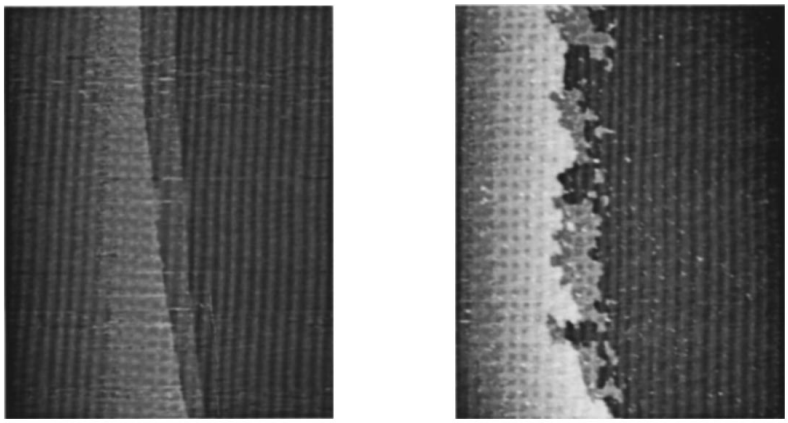

FIG. 9. A preadsorbed O overlayer inhibits the formation of pits: (a) Clean surface (3000 Å$\times$4000 Å) with wide terraces $\sim$1000 Å . (b) The same surface area, first covered by a $\sim(4\times1)$-O overlayer, and then exposed to an oxygen pressure of $\sim10^{-5}$ mbar. Steps become ''roughened'' only after the oxygen pressure is increased to 10^{-5} mbar. No pits form on the large terraces due to the preexisting O overlayer.

rate contributes a reduced concentration of adatoms on larger terraces than on smaller terraces. This leaves more excess diffusing oxygen atoms to create vacancies on larger terraces. As noted previously, a vicinal Ag(110) surface with a mean terrace width less than 100 Å simply facets[4] at $P_c\sim10^{-5}$ mbar with no evidence of pit formation.

Clearly, the model used to derive the critical pressure oversimplifies the many complicated processes that may accompany pit formation. To estimate P_c, we assumed that the detached Ag atoms distribute across the terrace very fast. We also assumed that during the mean detachment time the formation of Ag-O nuclei is complete. That is, we assumed Ag adatoms diffuse quickly and react to completion with oxygen to form Ag-O nuclei. The first assumption *overestimates* the critical pressure since, if diffusion is slow, lower oxygen pressures will suffice to deplete the Ag adatoms. The second assumption *underestimates* the critical pressure since, if the Ag-O formation is slow, higher oxygen pressures are needed to increase the nucleation rate. Apparently, these effects either cancel, or are unimportant, as Eq. (3) leads to an experimentally observable result. Of course, additional information of such a complex process as pit formation calls for further investigation of such microscopic phenomena as rates for diffusion, Ag-O nucleation, added-row formation, and pit formation.

Finally, we note with some surprise that the pits observed on O/Ag(110) are as large as several hundred Å in diameter. Furthermore, the rather round shapes of the vacancy islands on Ag(110) (see Fig. 8) are far from the highly eccentric elliptical shape[26] predicted at equilibrium by the very different stiffness of [110] and [001] steps.[27] Clearly, nonequilibrium kinetics are involved in the generation of pits. For O/Cu(110) and O/Ni(110), pit formation was also observed. Pits start to form on O/Cu(110) when the surface is roughly covered by 50% of (2×1)-O islands.[28] The (2×1)-O islands block transport of Cu adatoms from the step edges onto the terraces and the pits form. For O/Ni(110), the formation of ''troughs'' and added rows proceeds in parallel.[12] These results are consistent with a reduced mobility of Ni adatoms on Ni(110) compared to Cu adatoms on Cu(110). The kinetic hindrance of silver transport by the added rows on Ag(110) does not contribute significantly to pit formation. As mentioned earlier (Fig. 9), pits will not form if the added-row structure is preestablished. Finally, we recall that the much higher adatom density on Ag(110) than on Cu(110) and Ni(110) distinguishes the added-row formation kinetics in these three systems at room temperature, as reported previously.[2]

V. CONCLUSION

The relationship between the formation of added rows and the mass transport mechanism at step edges has been examined quantitatively for the O/Ag(110) system. Strong evidence that O/Ag(110) adopts an added-row structure, in which O atoms incorporate additional Ag adatoms into Ag-O-Ag chains along [001], is presented. These added rows exhibit substantial mobility, unless stabilized by ''pinning'' mechanisms. The additional Ag adatoms needed for added rows are readily supplied by the step edge via thermal detachment at a nominal rate of three atoms/s at room temperature, and mobile Ag adatoms are shown to exist on terraces even prior to oxygen exposure. At oxygen pressures below a critical pressure of 10^{-5} mbar, the supply of Ag adatoms from the step edges suffices for the formation of oxygen overlayers, and is not rate limiting. At $P\geqslant10^{-5}$ mbar, the formation of oxygen overlayers is sustained by the creation of pits on the large (110) terraces, revealing a second ''substrate extraction'' channel for Ag adatoms, in addition to the step-edge supply. We are able to predict this critical pressure by considering the kinetic competition between the supply rate from step edges and the overlayer formation rate on terraces. The sensitivity of the kinetic mechanism for oxygen overlayer formation to oxygen pressure is a clear example of a ''pressure gap'' in the oxidation of Ag(110).[29] Finally, the mass transport mechanism at Ag(110) steps provides reactive nucleation centers, i.e., the mobile Ag adatoms, distributed across the terraces. The reaction sites during oxidation are thus distributed across the terraces, not localized at steps.

ACKNOWLEDGMENTS

W.W.P. acknowledges support by NSF-MRG Grant No. DMR91-03031. J.E.R.R. acknowledges support by NSF Grants No. CHE-9303062, No. CHE-9157467, the Packard Foundation, and the Sloan Foundation. We especially acknowledge the interest and insight of N. C. Bartelt.

*Present address: Solid State Division, Oak Ridge National Laboratory, Oak Ridge, Tennessee.

[1] G. A. Somorjai and M. A. Van Hove, Prog. Surf. Sci. **30**, 201 (1989).

[2] T. Hashizume, M. Taniguchi, H. Lu, K. Tanaka, and T. Sakurai, Jpn. J. Appl. Phys. **30**, L1529 (1991); W. W. Pai, N. C. Bartelt, M. Peng, and J. E. Reutt-Robey, Surf. Sci. Lett. **330**, L679 (1995).

[3] J. S. Ozcomert, W. W. Pai, N. C. Bartelt, and J. E. Reutt-Robey, Surf. Sci. **293**, 183 (1993).

[4] J. S. Ozcomert, W. W. Pai, N. C. Bartelt, and J. E. Reutt-Robey, Phys. Rev. Lett. **72**, 258 (1993).

[5] H. A. Engelhardt and D. Menzel, Surf. Sci. **57**, 591 (1976).

[6] These variations, previously reported by M. Taniguchi, K. I. Tanaka, T. Hashizume, and T. Sakurai, Surf. Sci. Lett. **262**, L123 (1992), have been described as a ''phase coexistence.'' Strictly speaking, the size of the ''domains'' (often <20 Å) is too small to support a true thermodynamic phase. Indeed, slight variations in coverage from the ideal phase [e.g., 0.22 ML for the (4×1)-O phase] force local variations in O chain densities.

[7] L. Becker, S. Aminpirooz, A. Schmalz, B. Hillert, M. Pedio, and J. Haase, Phys. Rev. B **44**, 13 655 (1991).

[8] L. Yang, T. S. Rahman, G. Biracco, and R. Tattarek, Phys. Rev. B **40**, 12 271 (1989).

[9] A. Puschmann and J. Hasse, Surf. Sci. **144**, 559 (1984).

[10] G. Bracco, C. Malo, C. J. Moses, and R. Tatarek, Surf. Sci. **287/288**, 871 (1993).

[11] D. J. Coulman, J. Wintterlin, R. J. Behm, and G. Ertl, Phys. Rev. Lett. **64**, 1761 (1990).

[12] L. Eierdal, F. Basenbacher, E. Lægsgaard, and I. Stensgaard, Surf. Sci. **312**, 31 (1994).

[13] T. Schimizu and M. Tsukada, Surf. Sci. Lett. **295**, L1017 (1993).

[14] A low-energy ion scattering experiment indicated the oxygen atoms sit below the top Ag layer by 0.03 Å [M. Canepa, P. Cantini, F. Fossa, L. Mattera, and S. Terreni, Phys. Rev. B **47**, 15 823 (1993)] instead. Recent STM measurements of O/Ag(110) by I. Stensgaard, E. Lægsgaard, and F. Besenbacher [J. Chem. Phys. **103**, 9825 (1995)] argue that Ag atoms, rather than O atoms, are imaged as protrusions with a tungsten tip. We also found occasionally that the oxygen chains appear as dark troughs. This contrast reversal is most likely due to the change of tip characteristics by oxygen adsorption [L. Ruan, F. Besenbacher, I. Stensgaard, and E. Læsgaard, Phys. Rev. Lett. **70**, 4079 (1993)]. The actual position of the O atoms remains to be resolved.

[15] The adsorption heat for the chemisorption of oxygen might cause thermal drift. However, by comparing the amount of step retraction for terraces with different widths, we conclude this effect is negligible.

[16] W. W. Pai, N. C. Bartelt, and J. E. Reutt-Robey, preceding paper, Phys. Rev. B **53**, 15 991 (1996).

[17] R. L. Schwoebel and E. J. Shipsey, J. Appl. Phys. **37**, 3682 (1966).

[18] Jacobsen and Nøskov have calculated the metal-oxygen hybridization energy with the embedded-atom method, finding the hybridization energy increases as the coordination number for the metal atom decreases [K. W. Jacobsen and J. K. Nøskov, Phys. Rev. Lett. **65**, 1788 (1990)]. It is then reasonable to expect the mobile Ag adatoms on the terraces are highly reactive during oxidation.

[19] L. Vattuone, M. Rocca, C. Borarno, and U. Valbusa, J. Chem. Phys. **101**, 713 (1994).

[20] The low density of oxygen at the initial stage of overlayer formation justifies the use of mean detachment time of the clean surface.

[21] Because the vibrational entropy is typically small, the energy ΔG_f is roughly the same as the formation energy ΔE_f for placing one bulk Ag atom on the surface.

[22] S. M. Foiles, Surf. Sci. Lett. **191**, L779 (1987).

[23] S. V. Khare and T. L. Einstein, Surf. Sci. **314**, L857 (1994).

[24] K. M. Ho and K. P. Bohnen, Phys. Rev. Lett. **59**, 1833 (1987).

[25] K. W. Jacobsen and J. K. Nøskov, Phys. Rev. Lett. **60**, 2496 (1988).

[26] N. C. Bartelt, R. M. Tromp, and E. D. Williams, Phys. Rev. Lett. **73**, 1656 (1994).

[27] W. W. Pai, N. C. Bartelt, and J. E. Reutt-Robey (unpublished).

[28] J. Wintterlin, R. Schuster, D. J. Coulman, G. Ertl, and R. J. Behm, J. Vac. Sci. Technol. B **9**, 902 (1991).

[29] K. Christmann, *Introduction to Surface Physical Chemistry* (Springer-Verlag, New York, 1991).